Research Article Vol. 27, No. 22 / 28 October 2019 / Optics Express 31956

Optics EXPRESS

User-defined microstructures array fabricated by DMD based multistep lithography with dose modulation

YING ZHANG,[1,5] JUN LUO,[1,5] ZHENG XIONG,[2] HUA LIU,[1,4] LI WANG,[3] YINGYING GU,[3] ZIFENG LU,[1] JINHUAN LI,[1] AND JIPENG HUANG[1]

[1] *Demonstration Center for Experimental Physics Education, College of Physics, Northeast Normal University, Changchun 130024, China*
[2] *Department of Biomedical Engineering and Chemical Engineering, Syracuse University, Syracuse, NY 13244, USA*
[3] *Lab of Space Optoelectronic Measurement and Perception, Beijing Institute of Control Engineering, China*
[4] *State Key Laboratory of Applied Optics, Changchun Institute of Optics, Fine Mechanics and Physics, Chinese Academy of Sciences, Changchun 130033, China*
[5] *Authors contributed equally to this work*
[*] *liuhua_rain@aliyun.com*

Abstract: A flexible and efficient strategy, digital micromirror devices (DMD) based multistep lithography (DMSL), is proposed to fabricate arrays of user-defined microstructures. Through the combination of dose modulation, flexible pattern generation of DMD, and high-resolution step movement of piezoelectrical stage (PZS), this method enables prototyping a board range of 2D lattices with periodic/nonperiodic spatial distribution and arbitrary shapes and the critical feature size is down to 600 nm. We further explore the use of DMSL to fabricate microlens array by combining with the thermal reflowing process. The square shape and hexagonal shape microlens with customized distribution are realized and characterized. The results indicate that the proposed DMSL can be a significant role in the microfabrication techniques for manufacturing functional microstructures array.

1. Introduction

Periodic/nonperiodic microstructures array has been extensively utilized in surface/interface engineering, microelectromechanical systems (MEMS), microoptoelectromechanical system (MOEMS), metasurface/metamaterials etc [1–6]. With different spatial distribution and shapes, these microstructures array can realize variously functional devices, such as antireflective surface, microlens array, metalenses, antiwetting surface and antimicrobial topography. Even if recent technological advances have enables prototyping these microstructures array in high-resolution or in large-area or in flexible spatial distribution, available fabrication strategies cannot fabricate new designs with required feature sizes both rapidly and at low cost. For instance, mask-based photolithography, nanoimprint lithography and microcontact printing are suited to high-throughput manufacturing but they still require high resolution physical masks [7–9]. And direct laser writing, electron-beam lithography, and ion-beam etching can offer high resolution even beyond diffraction-limitation, while they are typically low production efficiency and expensive [10–13]. None of these techniques above can efficiently and flexibly fabricate user-defined microstructures array during the iterating new designs between theorical simulation and actual manufacturing.

Recently, maskless photolithography has attracted widespread attention as it is an efficient manufacture technology. For representative example, interference photolithography provides

#372953 https://doi.org/10.1364/OE.27.031956
Journal © 2019 Received 25 Jul 2019; revised 12 Sep 2019; accepted 15 Sep 2019; published 18 Oct 2019

a facile, inexpensive, large scale-lithography. However, it is limited to fabricating periodic structures array. As promising alternative, spatial light modulator-based projection lithography especially DMD based lithography [14–22], due to the flexible pattern generation of DMD, provides rapid processing speed and is suitable for manufacturing large-area periodic/nonperiodic microstructures. Yet, the conventional DMD based lithography is still limited in the resolution of submicron scale. To overcome this limitation, researchers have used high de-magnification projection lens. However, there is a trade-off between exposure area and minimum feature size, that is, to obtain the minimum width, the loss of exposure area needs to be considered. In addition, the conventional DMD based lithography system is static, that is, the DMD device and the exposure substrate are static. The spatial distribution or the period of the microstructures array is constrained by the period of the DMD's micromirrors. The customized distribution of the microstructures array, for example, if the desired period of microstructures array is not the integer times of the period of DMD's micromirrors, it is impossible to be realized using the conventional system. Therefore, it is highly desirable to develop a flexible lithography technique that is capable to fabricate user-defined microstructures array rapidly and at low cost.

To address these challenges, we propose a new developed DMD based multistep lithography (DMSL) technique, which combines the dose modulation, the high-resolution movement of PZS, and the flexible pattern generation of DMD, to achieve user-defined microstructures array. We demonstrate that the DMSL can be used to fabricate cross-shape array with 2D period, dots matrix with hexagonal period and nonperiodic C-shape array. Furthermore, by combining with thermal reflowing process, this work demonstrates the capability to fabricate functional microlens array with user-defined shapes and periods.

2. Methods

2.1. Experimental setup

The schematic of the proposed DMSL system is shown in Fig. 1. In this system, UV light source with central wavelength of 405 nm is used, which is homogenized and collimated by customized illumination system. After being collimated and expanded, the light beam illuminates on digital micromirror device (DMD, Texas Instruments Inc.). The DMD used in this system consists of an array of 1024×768 micromirrors with single pixel size of 13.68 µm. Each mirror can be switched between light reflecting "on" (+12°) and "off" (−12°) directions which is modulated by input pattern (Fig. 1(i)) to create specific spatial intensity profile (Fig. 1(ii)). After being modulated, the pattern on DMD is projected through the de-magnified imaging system which includes tube lens (1×, Edmund Optics) and objective (10×, Edmund Optics), and then projected onto a glass substrate spin coated with 1 µm thickness photoresist (S1813). The target glass substrate is positioned on a piezoelectric stage (PZS). Here, the proposed system is different with conventional DMD based projection lithography system where the target sample is positioned on static stage. We take advantage of the high-resolution property of PZS (maximum moving range 100 um, resolution 7 nm) to achieve multistep exposure (Fig. 1(iii)) through step movement (which will be presented in detail in section 2.3). Besides, based on the dose modulation, the feature size can be decreased to submicron resolution (which will be presented in detail in section 2.2). With this exposure modality and taking use of flexible pattern generation of DMD, we could achieve user-defined periodic/nonperiodic microstructures array.

2.2. Dose modulation to realize sub-pixel resolution

In the static DMD based projection lithography, the feature size is determined by the demagnification ratio of the projection lens. For instance, if we use the same 10× objective as the one used in the proposed system, the smallest feature size is 1.368 µm in the static DMD system. To achieve sub-pixel resolution, the objectives with higher demagnification ratio such as 20× are

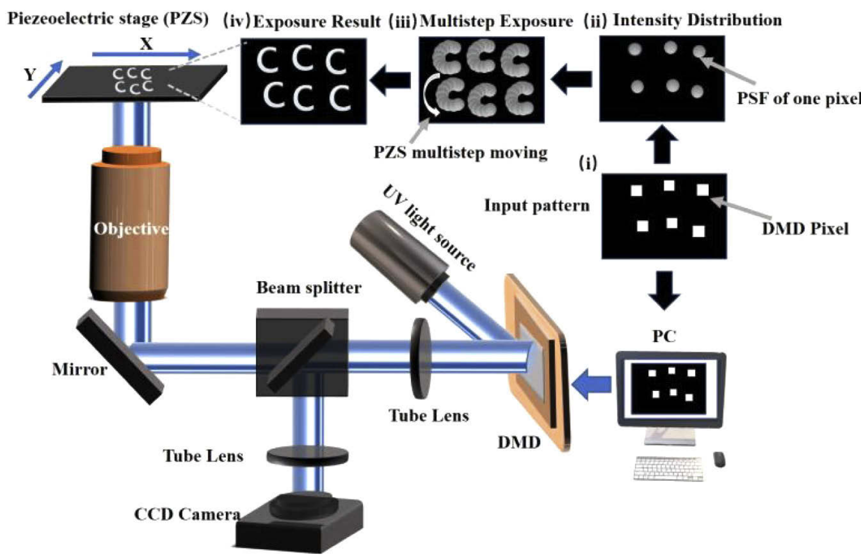

Fig. 1. Schematic of DMD based multistep lithography system including UV light source, DMD, tube lens, beam splitter, mirror, objective, piezoelectric stage (PZS) and CCD camera. User-defined dot array pattern (i) was inputted into DMD where each pixel corresponds to intensity distribution (ii). Through multistep movement of PZS (iii), final exposed structure (iv) was formed on the photoresist.

required. However, there is a tradeoff between the exposure area and the smallest feature size, i.e., to obtain the possible minimum size, the loss of the exposure area needs to be considered. In our proposed DMSL, the smallest feature size is not limited by the demagnification ratio of projection optics. Considering the photoresist threshold is constant, the feature size could be decreased through modulating exposure dose so that fabricating sub-pixel structures is feasible. To investigate the relationship between dose modulation of each DMD pixel and the feature sizes, the intensity profile of each DMD pixel could be simplified as a 2D Gaussian function.

$$\mathrm{I(x, y)} = \mathrm{I_0 e}^{-\left[\left(\frac{x}{a}\right)^2+\left(\frac{y}{b}\right)^2\right]} \tag{1}$$

where I(x, y) is the intensity profile of each DMD pixel on photoresist, $\mathrm{I_0}$ is the peak intensity, and a, b is the length and the width of each DMD pixel.

The final exposure dose on the photoresist is relative with the intensity profile and the exposure time.

$$\mathrm{D} = \mathrm{I(x, y)} \times \mathrm{T} \tag{2}$$

where D is the exposure dose of each pixel, and T is the exposure time.

According to Eq. (1) and Eq. (2), we simulated the final exposure dose on the photoresist using MATLAB software as shown in Fig. 2. Here, we assume that the threshold of the photoresist is constant. The exposure dose above the threshold determines the feature size which is calculated at the full width at half maximum (FWHM). The top view and side view in Fig. 2 show that the width is gradually decreased as the exposure dose decreases. Based on this modality, it is feasible that the feature size could be smaller than the size decided by the demagnification ratio.

2.3. Multistep lithography based on the high-resolution step movement of PZS

To achieve arbitrary microstructures array with user-defined spatial distribution and customized shape (including dot matrix in section 3.1, section 3.2 and continuous microstructures in

Optics EXPRESS

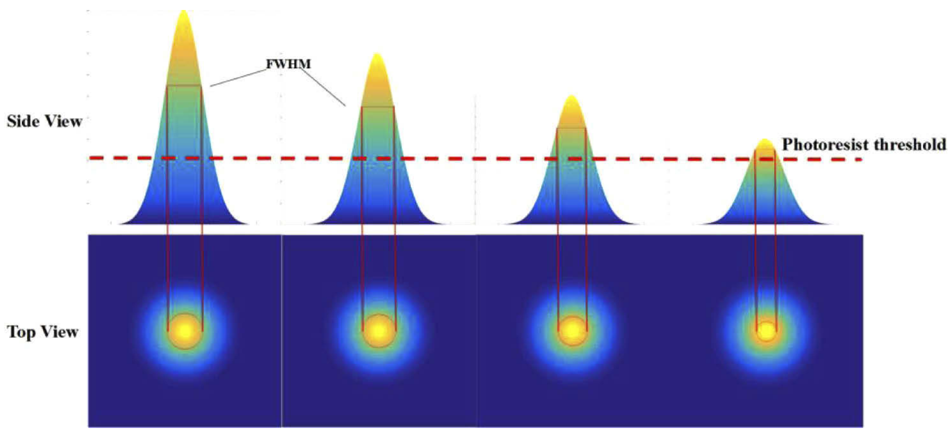

Fig. 2. Simulation result of dose modulation. With decreasing exposure dose, the FWHM of intensity profile above the photoresist threshold is decreased and the subpixel resolution is realized.

section 3.3), we propose a multistep lithography technique that transfer the conventionally static DMD lithography system to a dynamic lithography system by integrating the high-resolution movement of PZS. The basic principle is shown in Fig. 3. Briefly, according to the desired microstructures which are dots matrix or cross-shape microstructures array, we design and input the initial pattern into DMD as the Fig. 3(A). Note that the actual intensity profile of each DMD pixel (Fig. 3(B)) is simplified as the Gaussian intensity profile which was described in section 2.2. For fabricating the microstructures array, the PZS is moved according to the desired pattern. After one step movement with constant distance "*d*", one pattern on DMD is exposed on the photoresist (Fig. 3(C)). After multistep movement and the corresponding exposure until passing through the moving path (the arrows in Fig. 3(C)) of desired pattern, the final intensity profile formed on the photoresist via multistep exposure is the intensity accumulation from the Gaussian intensity of each step (Fig. 3(C)). After the development of the photoresist, the final microstructures are formed on the substrate (Fig. 3(D)). Figure 3(E) illustrates the actual exposure results of the microstructures array. Note that the moving distance "*d*" of each step determines the fabrication of continuous and discontinuous microstructures array. With large moving distance, the discontinous microstructures are fabricated as the dots matrix shown in the

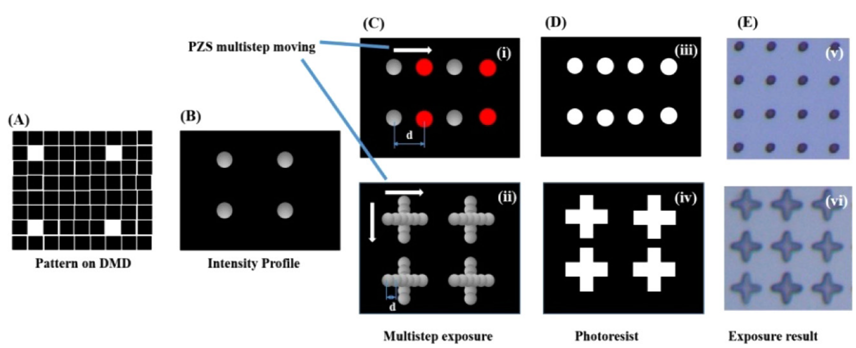

Fig. 3. Schematic of multistep lithography. (A) Pattern on the DMD, which corresponds to (B) intensity profile of each DMD pixel on the photoresist. With (C) PZS multistep moving, the (D) multistep exposure is formed on the photoresist (E) are actual exposure results characterized under Olympus bright-field microscope.

Optics EXPRESS

Fig. 3(E)-(v). With small moving distance, the continuous microstructures are manufactured as the cross-shape microstructure shown in the Fig. 3(E)-(vi) and the further exposure results will be presented in section 3.3. Further exploration of the moving distance for realizing the customized spatial distribution of microstructures array will be presented in section 3.1.

3. Fabrication of user-defined microstructures array by using DMSL with combined techniques

To achieve the user-defined microstructures array, we combine three main techniques including flexible pattern generation, multistep lithography and dose modulation into DMSL. The main procedure for achieving the user-defined microstructures array based on the technique combination is presented in the flow chart Fig. 4. Briefly, according to the desired microstructures array, we firstly extract two important information, that are, the spatial distribution of the array which is helpful to design the initial pattern for DMD, and the shape of microstructure which is fitted in MATLAB to get the graphic function, $y = f(x)$. The initial pattern and the graphic function determine the digital mask on DMD and the moving path of PZS, respectively. Then we take three applications as the examples to illustrate the techniques combination. In section 3.1, the microdots matrix with user-defined periods is fabricated through the combination of flexible pattern generation and the multistep lithography under large step movement. In section 3.2, further integration of dose modulation into the combination in section 3.1 leads to submicrodots matrix. In section 3.3, the microstructures arrays with user-defined shape and customized spatial distribution are realized by the combination of flexible pattern generation and the multistep lithography under small step movement. All details will be presented in the following sections.

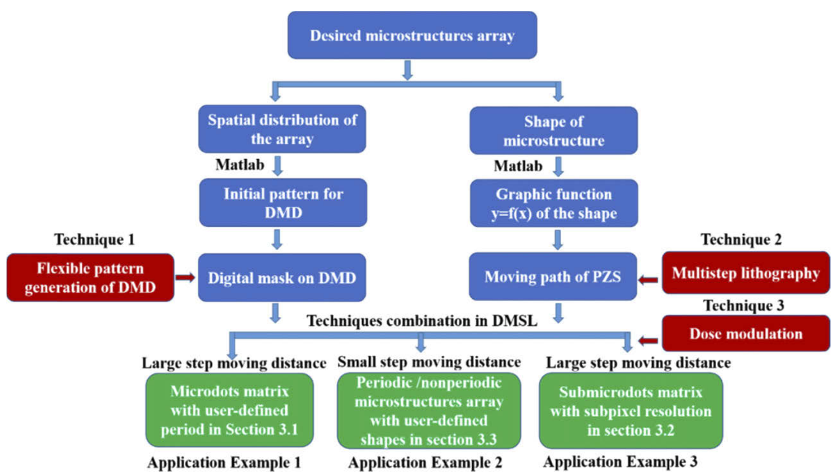

Fig. 4. Flow chart of techniques combination in DMSL and the application examples in this paper. The blue charts illustrate the process of achieving user-defined microstructures array. The red charts represent the three main techniques applied in the DMSL. The green charts are the application examples in 3.1, 3.2 and 3.3.

3.1. Fabrication of microdots matrix with user-defined period

We demonstrated in section 2.3 that DMSL can be exploited to realize customized periodic microstructures array by taking use of the flexible generation of DMD and the high-resolution movement of PZS. Here, we fabricate microstructures array with arbitrary hexagonal period. The further explanation on how to fabricate it is shown in Figs. 5(A) and 5(B). Note that the pitch size of the grid in these figures represents the period of DMD pixels which is "D" (1.368 μm).

The interval between the two adjacent dots represents the desired period which is d. Here we design the desired microstructures array with "d" as 3 µm. Then we obtain the initial pattern as these black points $A_{0,\,0}$ in Fig. 5(A) for the digital mask shown on DMD. To guarantee the periodic property of microstructures array, the relationship between DMD pixel period "D" and the desired period of microstructures array "d" needs to follow Eq. (3).

$$\begin{cases} N_1 \times d = N_2 \times D \text{ (along y direction)} \\ N_3 \times \sqrt{3}d = N_4 \times D \text{ (along x direction)} \end{cases} \tag{3}$$

Where N_1, N_2, N_3 and N_4 should be integer, d is the moving distance of PZS and is defined as the desired period, and D is the period of DMD pixel, which is 1.368 µm here.

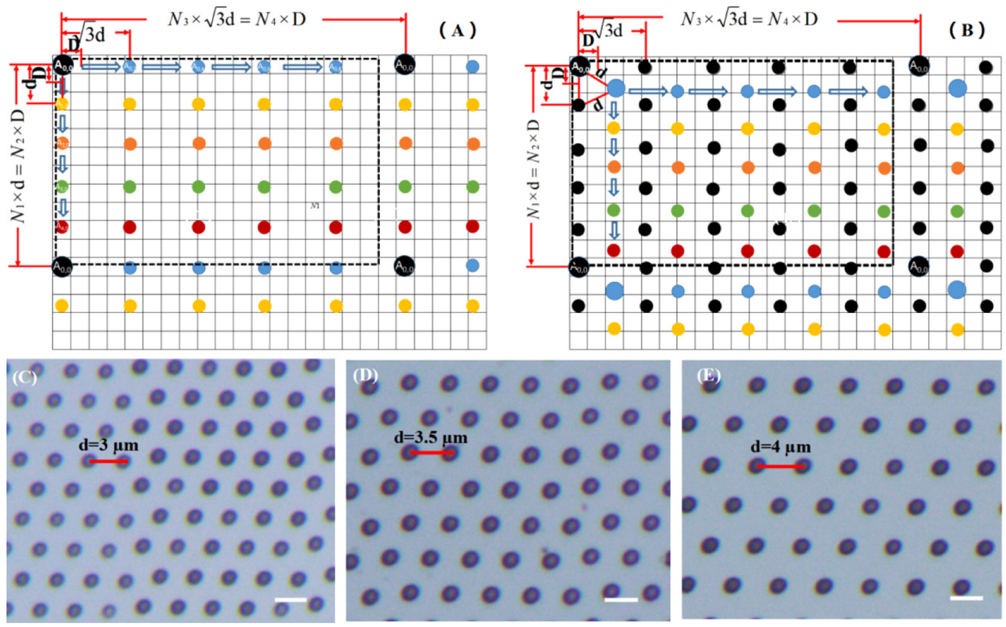

Fig. 5. (A) and (B) schematic of multistep lithography to achieve dots matrix and (C)-(E) the brightfield images of the actual exposure results with different periods. Scale bar: 3 µm.

We first make PZS implement multistep movement in x and y directions by using the arrows in Fig. 5(A) as the moving path. With each step movement, the corresponding exposure experiment is implemented on the substrate. The all dots matrix presents the exposure results. And further step movement is necessary for realizing hexagonal periodic microstructures array. Thus, we move the initial position of $A_{0,\,0}$ by $\frac{\sqrt{3}d}{2}$ and $\frac{d}{2}$ on x and y directions, respectively. Then the PZS is implemented the multistep movement following the same moving path as Fig. 5(A) on x and y directions until finishing all desired microstructures fabrication. Finally, we obtained a hexagonal period of microstructures array with a preset period of 3 µm (Fig. 5(B)). With this modality, we have implemented the actual exposure experiments on the glass substrate with 1 µm thickness positive photoresist (S1813). We realized the periodic microstructures with different hexagonal periods (3 µm, 3.5 µm and 4 µm) in Figs. 5(C)–5(E).

3.2. Fabrication of submicrodots matrix with subpixel resolution

In section 3.1, we have demonstrated the fabrication of customized hexagonal microdots matrix with feature size around 1.3 µm. Here, we further explore the DMSL fabrication technique by

Optics EXPRESS

combining with the dose modulation technique described in section 2.2 by using 10× objective lens. The quantified relationship between the exposure dose and feature size is presented in Fig. 6(A) where we modulate the dose through tuning the exposure time and the UV light source intensity. As Fig. 6(A) shows, the feature size is increased to almost 1.8 µm with increasing the exposure dose. And the smallest feature size is down to 0.6125 µm with decreasing the exposure dose. This size is almost half of the critical feature size (1.368 µm) of which fabricated by using conventional DMD lithography system. Figure 6(B) presents the actual exposure results on the photoresist, which are characterized by Olympus brightfield microscope. Figs. 6(C) and 6(D) are the SEM images of the micro/submicro dots matrix under 1.4 mW with 2 s and 1 s respectively. Therefore, these results indicate that the dose modulation is an efficient method for achieving sub-pixel resolution without losing the exposure area. It is expected that further dose modulation can be helpful to realize smaller feature size.

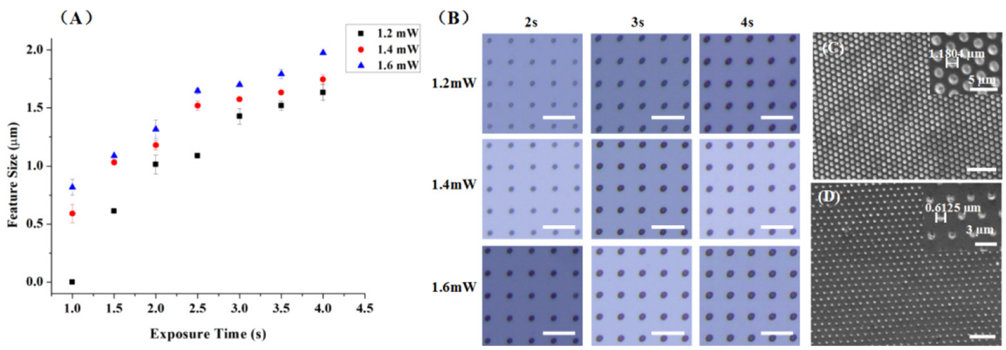

Fig. 6. (A) The diagram of feature size and exposure dose (intensity and exposure time). (B) Brightfield microscope images of micro/submicro dots matrix with different intensity and exposure time. (C) and (D) Micro/submicrodots matrix fabricated under 1.4 mW, 2 s/1 s exposure dose and characterized by SEM. Scale bar: 10 µm.

3.3 Fabrication of periodic/nonperiodic microstructures array with user-defined shape

In section 2.3, we have presented that the DMSL can be used to fabricate continuous microstructures array when the moving distance of each step is small enough. Here, we implement DMSL under micron-scale step movement and combines it with the flexible pattern generation of DMD to realize user-defined periodic/nonperiodic microstructures. For this target, we firstly optimize the moving distance through MATLAB simulation (Figs. 7(A)–7(D)) using the Gaussian model in section 2.2 and actual exposure experiments (Figs. 7(E)–7(H)) during which the exposure intensity and the exposure time are fixed at 1.4 mW and 1 s respectively. We found that the optimum distance is 1.1 µm with which the fabricated line is continuous, and the width of the line is 0.6806 µm which is only increased by 0.07 µm compared with the feature size which the single DMD pixel exposed and got (0.6125 µm). Therefore, we will use this distance, the exposure intensity and the exposure time to fabricate the microstructures in this section and section 4.

After the optimization of the step moving distance, we use the optimized parameter to fabricate the customized microstructures array. Based on the flow chart in Fig. 4, we first get the initial pattern (inset in Figs. 8(A) and 8(E)) on DMD according to the spatial distribution of the desired microstructures array. And then the graphic function of the desired microstructure $y = f(x)$ provides the moving path of PZS as the arrows in Figs. 8(A) and 8(E). With all the information above, we implemented the simulation using MATLAB based on the Gaussian model described in section 2.2 and the results are presented in Figs. 8(B) and 8(F). Then we fabricated the periodic microstructures array. The length and the width microstructures with cross-shape are

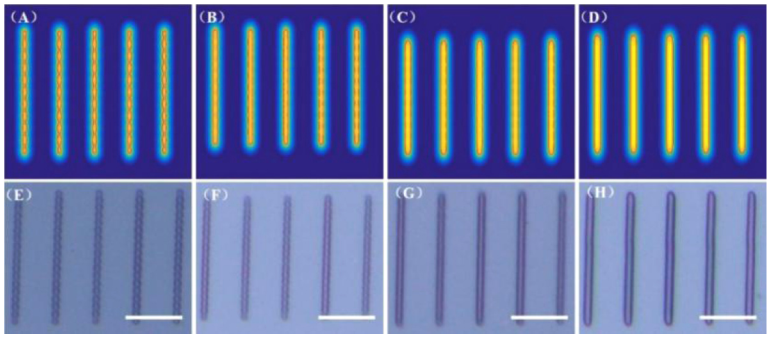

Fig. 7. Simulation (A-D) and fabrication (E-H) of lines pattern with different moving step (1.3 µm, 1.2 µm, 1.1 µm and 1.0 µm). Scale bar: 10 µm.

5.0468 µm. The actual exposure results were characterized under brightfield microscope and SEM in Figs. 8(C) and 8(D) respectively. There is a thicker profile at the concave corners of the cross-shape structures compared with the simulated results. This results from the intensity overlapping among adjacent exposure dots. Here we combine the flexible pattern generation of DMD and further exploit the DMSL to fabricate the nonperiodic microstructures array with C-shape. The intial pattern of nonperiodic distribution is automatically obtained through customized random function programmed in MATLAB (Fig. 8(E)). The graphic function of the C-shape is fitted using MATLAB polynomial function which is $f(x) = x^2 - 4.104x + 4.104$ $(0 \leq x \leq 4.104)$. By using this function as moving path (Fig. 8(F)), we realized the desired microstructures as shown in Figs. 8(G) and 8(H). The length and width of the C-shape microstructure are 5.6216 µm and 4.2925 µm, respectively.

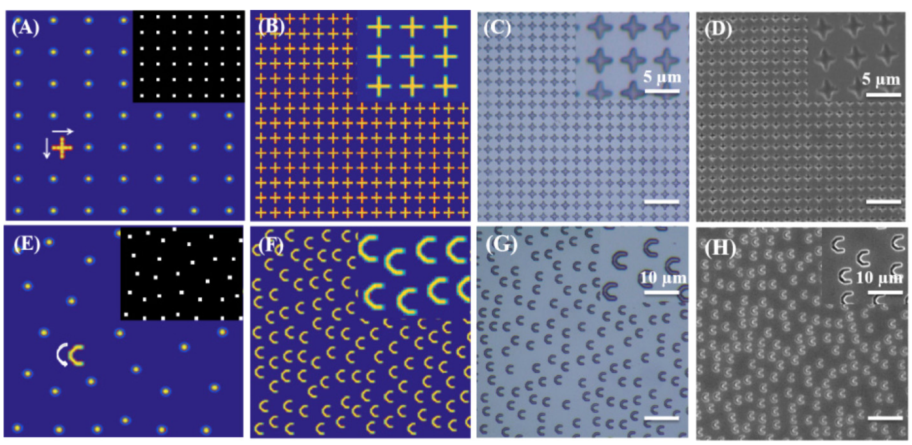

Fig. 8. User-defined period and nonperiodic microstructures arrays fabricated by DMSL with combined techniques. (A) and (E) initial pattern and moving path. (B) and (F) the exposure results are simulated in MATLAB. (C) and (G) the actual exposure results characterized under Olympus microscope. (D) and (H) the acutal exposure results characterized under SEM. Scale bar: 20 µm.

4. Fabrication of user-defined microlens array

Based on the technique combination in the proposed DMSL, we have demonstrated the capability of DMSL to fabricate arbitrary microstructures array. Here, we explore the DMSL further and

Optics EXPRESS

combine it with thermal reflowing process to achieve functional microlens array. Compared with the microlens array fabricated by using the conventionally static DMD lithography, the period of microlens array fabricated by our proposed DMSL will be not constrained with the period of DMD's micromirrors as described in section 3.1. Furthermore, with the integration of dose modulation, we can decrease the size of the gap between two microlens so that achieve high fill-factor microlens array [23]. With the combination of the flexible pattern generation of DMD and the multistep lithography by using PZS, we can realize customized spatial distribution of microlens array and user-defined shape of microlens.

According to the flow chart in Fig. 4, we extracted the initial pattern as the dots matrix shown in Figs. 9(A), 9(E) and 9(I) and the moving path of PZS as the arrows shown in these figures respectively from the desired microlens array. Based on the Gaussian model in section 2.2, we simulated the exposure results using MATLAB software. The results are presented in Figs. 9(B), 9(F) and 9(J). The actual exposure results are implemented on glass substrate with spin-coated positive photoresist. The exposure experiments under the same exposure intensity 1.4 mW and exposure time 1s used in section 3. And the exposed substrate is developed in 5‰ (w/v) NaOH solution for 3 seconds to remove the reacted photoresist. After the development, the exposed substrate is characterized under Olympus bright-field microscope as shown in Figs. 9(C), 9(G) and 9(K). Then the developed substrate is inverted on the hot plate under 180 ° C with 20 s for the thermal reflowing process [24]. The fabricated microlens arrays after the thermal reflowing process are characterized under SEM. We found that the gap between the microlens is covered after the thermal reflowing even if there was the gap 0.7486 µm before thermal reflowing process as shown in Figs. 9(C) and 9(G). Thus, the fill factor of the microlens array is almost 100% as shown in Figs. 9(D) and 9(H). We realized the square-shape, hexagonal shape microlens array with period 9.576 µm and 6.81 µm respectively by combing the flexible pattern generation with multistep lithography. Furthermore, we exploited the techniques combination and achieved the microlens array with customized spatial distribution according to the university LOGO "NENU" as shown in Fig. 9(L).

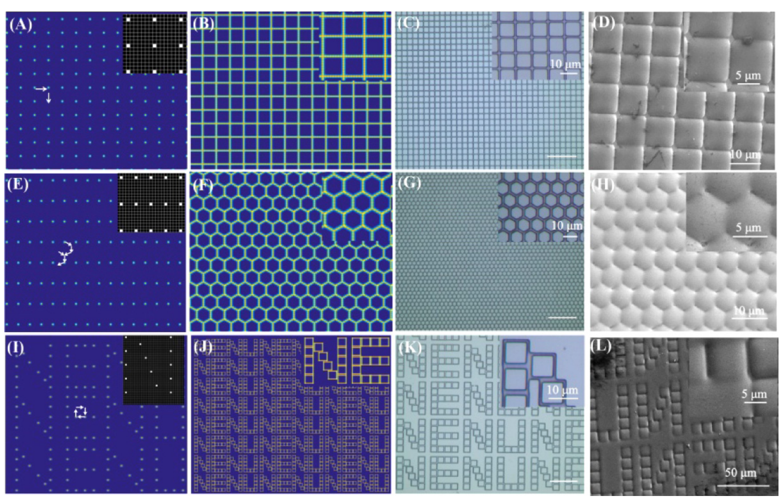

Fig. 9. Fabrication of microlens array with user-defined shape (square-shape, hexagonal shape) and customized spatial distribution (2D period, hexagonal period and nonperiod). (A), (E) and (I) represent the initial pattern on DMD. (B), (F) and (J) presents the simulated exposure results using Gaussian model. (C), (G) and (K) presents the exposed substrate before thermal reflowing process characterized under Olympus bright-field microscope. (D), (H) and (L) present microlens arrays after thermal reflowing process characterized under SEM. Scale bar: 50 µm

Optics EXPRESS

To further verify the functionality of these fabricated microlens array, the characterization was implemented by using positive and negative photomask "A", pinhole and resolution test target, respectively. We characterized their optical imaging quality by using Olympus bright-field microscope where we put the three targets above the light source as shown in Fig. 10(A). The microlens arrays perform sharp imaging under positive and negative photomask as shown in Figs. 10(B) and 10(C). And the periodic microlens array and nonperiodic microlens array "NENU" shows very good focusing property as the focal spot image in Figs. 10(D) and 10(E). Furthermore, the microlens array shows a great resolving property as it can resolve the resolution test target with 12.7 lp /mm, as shown in Fig. 10(F). All these results above indicate that the proposed DMSL can be used to fabricate customized functional microlens array and might be exploited in the future for manufacturing other functional microstructures array.

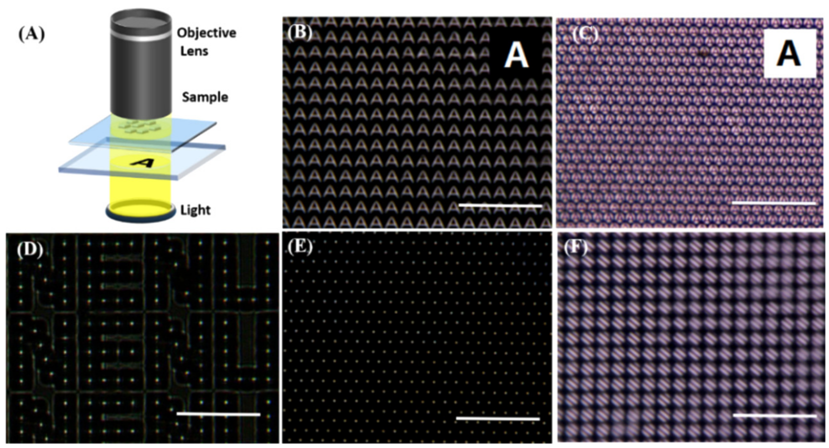

Fig. 10. Imaging quality characterization of user-defined microlens array. (A) Schematic of the characterization system using Olympus microscope. (B) Imaging quality of square-shape microlens array with 2D period array characterized by using positive photomask. (C) Imaging quality of Hexagonal shape microlens array with hexagonal period. (D) and (E) Focus spot image characterized by using pinhole. (F) Resolution test characterized by 12.7 lp/mm resolution target. Scale bar: 50 µm

5. Conclusion

In this paper, we proposed a new developed DMSL dynamic lithography system for efficient fabrication of user-defined microstructures array. By combing the flexible pattern generation of the DMD with the high-resolution movement of PZS, the proposed DMSL enabled rapid prototyping customized periodic/nonperiodic microstructures arrays. We further integrate the dose modulation technique in DMSL to achieve subpixel resolution which is down to 600 nm without sacrificing the exposure area. Moreover, combined with thermal reflowing process, DMSL was applied in fabricating high fill-factor microlens array with user-defined shape and spatial distribution. We characterized the imaging quality of these microlens arrays. The results of characterization demonstrate that the DMSL can be a promising technique for fabricating user-defined and functional microstructures array.

Funding

National Natural Science Foundation of China (No. 61875036); Jilin Scientific and Technological Development Program (20190302049GX).

Optics EXPRESS

Acknowledgments

The work described in this paper is supported by the State Key Laboratory of Applied Optics, and the Lab of Space Optoelectronic Measurement & Perception (LabSOMP-2018-05). We thank Zheng Xiong from Syracuse University who designed the framework of the article and took a leading role in writing the manuscript.

Disclosures

The authors declare no conflicts of interest.

References

1. Z. M. Zhang, Y. Q. Gao, N. N. Luo, K. L. Zhong, and Z. H. Liu, "Multi-direction digital moving mask method for fabricating continuous microstructures," Opt. Appl. **61**(1), 79–99 (2015).
2. R. Yang, S. A. Soper, and W. J. Wang, "Microfabrication of pre-aligned fiber bundle couplers using ultraviolet lithography of SU-8," Sens. Actuators, A **127**(1), 123–130 (2006).
3. C. J. Ke, X. J. Yi, Z. M. Xu, and J. J. Lai, "Monolithic integration technology between microlens arrays and infrared charge coupled devices," Opt. Laser Technol. **37**(3), 239–243 (2005).
4. C. Q. Yi, C. W. Li, S. L. Ji, and M. S. Yang, "Microfluidics technology for manipulation and analysis of biological cells," Anal. Chim. Acta **560**(1-2), 1–23 (2006).
5. X. Zhang, X. N. Jiang, and C. Sun, "Micro-stereolithography of polymeric and ceramic microstructures," Sens. Actuators, A **77**(2), 149–156 (1999).
6. C. Sun and X. Zhang, "The influences of the material properties on ceramic micro-stereolithography," Sens. Actuators, A **101**(3), 364–370 (2002).
7. M. A. Verschuuren, M. W. Knight, M. Megens, and A. Polman, "Nanoscale spatial limitations of large-area substrate conformal imprint lithography," Nanotechnology **30**(34), 345301 (2019).
8. H. Schift, "Nanoimprint lithography: an old story in modern times? A review," J. Vac. Sci. Technol. B **26**(2), 458–480 (2008).
9. M. A. Verschuuren, M. Megens, Y. F. Ni, H. V. Sprang, and A. Polman, "Large area nanoimprint by substrate conformal imprint lithography (SCIL)," Adv. Opt. Technol. **6**(3-4), 243–264 (2017).
10. A. Zukauskas, M. Malinauskas, C. Reinhardt, B. N. Chichkov, and R. Gadonas, "Closely packed hexagonal conical microlens array fabricated by directlaser photopolymerization," Appl. Opt. **51**(21), 4995–5003 (2012).
11. T. Kohoutek, M. A. Hughes, J. Orava, M. Mastumoto, T. Misumi, H. Kawashima, T. Suzuki, and Y. Ohishi, "Direct laser writing of relief diffraction gratings into a bulk chalcogenide glass," J. Opt. Soc. Am. B **29**(10), 2779–2786 (2012).
12. M. Malinauskas, A. Žukauskas, V. Purlys, A. Gaidukevičiu, Z. Balevičius, A. Piskarskas, C. Fotakis, S. Pissadakis, D. Gray, and R. Gadonas, "3D microoptical elements formed in a photostructurable germanium silicate by direct laser writing," Opt. Lasers Eng. **50**(12), 1785–1788 (2012).
13. Q. Yang, S. Tong, F. Chen, Z. Deng, H. Bian, G. Du, J. Yong, and X. Hou, "Lens-on-lens microstructures," Opt. Lett. **40**(22), 5359–5362 (2015).
14. Z. Xiong, H. Y. Li, P. Kunwar, Y. Zhu, R. Ramos, S. Mcloughlin, T. Winston, Z. Ma, and P. Soman, "Femtosecond laser induced densification within cell-laden hydrogels results in cellular alignment," Biofabrication **11**(3), 035005 (2019).
15. B. Yang, J. Y. Zhou, Q. M. Chen, L. Lei, and K. H. Wen, "Fabrication of hexagonal compound eye microlens array using DMD-based lithography with dose modulation," Opt. Express **26**(22), 28927–28937 (2018).
16. P. Kunwar, Z. Xiong, Y. Zhu, H. Y. Li, A. Filip, and P. Soman, "Hybrid laser printing of 3D, multiscale, multimaterial hydrogel structures," *Adv. Opt. Mater.* 1900656 (2019).
17. K. Totsu, K. Fujishiro, S. Tanaka, and M. Esashi, "Fabrication of three-dimensional microstructure using maskless gray-scale lithography," Sens. Actuators, A **130-131**, 387–392 (2006).
18. A. Rammohan, P. K. Dwivedi, R. Martinez-Duarte, H. Katepalli, M. J. Madou, and A. Sharma, "One-step maskless grayscale lithography for the fabrication of 3-dimensional structures in SU-8," Sens. Actuators, B **153**(1), 125–134 (2011).
19. A. Waldbaur, B. Waterkotte, K. Schmitz, and B. E. Rapp, "Maskless projection lithography for the fast and flexible generation of grayscale protein patterns," Small **8**(10), 1570–1578 (2012).
20. K. Kim, S. Han, J. Yoon, S. Kwon, H. K. Park, and W. Park, "Lithographic resolution enhancement of a maskless lithography system based on a wobulation technique for flow lithography," Appl. Phys. Lett. **109**(23), 234101 (2016).
21. Z. Xiong, H. Liu, X. Q. Tan, Z. W. Lu, C. X. Li, L. W. Song, and Z. Wang, "Diffraction analysis of digital micromirror device in maskless photolithography system," J. Micro/Nanolithogr., MEMS, MOEMS **13**(4), 043016 (2014).
22. Z. Xiong, H. Liu, R. H. Chen, J. Xu, Q. K. Li, J. H. Li, and W. J. Zhang, "Illumination Uniformity Improvement in Digital Micromirror Devices based Scanning Photolithography System," Opt. Express **26**(14), 18597–18607 (2018).
23. S. Z. Huang, M. J. Li, L. G. Shen, J. F. Qiu, and Y. Q. Zhou, "Fabrication of high quality aspheric microlens array by dose-modulated lithography and surface thermal reflow," Opt. Laser Technol. **100**, 298–303 (2018).
24. M. Wang, W. Yu, T. Wang, X. Han, E. Gu, and X. Lie, "A novel thermal reflow method for the fabrication of microlenses with an ultrahigh focal number," RSC Adv. **5**(44), 35311–35316 (2015).